Antimicrobial activity of microgels with immobilized copper(II) complex linked to crosslinking and composition

Babloo Sharma,‡ Carlie M. Clem,‡ Alda Diaz Perez, and Susanne Striegler*

Department of Chemistry and Biochemistry, 345 North Campus Drive, University of Arkansas, Fayetteville, AR, 72701, United States

KEYWORDS. Antimicrobial, Staphylococcus aureus, bactericidal, microgels, crosslinked poly(acrylate)s, binuclear copper(II) complex.

ABSTRACT: The resistance of many bacteria against currently available antimicrobial agents is increasing world-wide at an alarming pace. The described structure-activity relationship study was prompted by the extraordinary ability of water-dispersed microgels to hydrolyze glycosidic bonds similar to building blocks of the peptidoglycan layer of Gram-positive bacteria. The results establish polyacrylate microgels with embedded copper(II) complex as antimicrobial agents. The systematic study reveals that *S. aureus* is susceptible to the microgels, while common commercial agents are found intermediate or resistant. In particular, a microgel with 60 mol% of crosslinking, $^{Cu_2L}P_{60\%}$, shows intriguing bactericidal activity at 1 µg/mL, while vancomycin requires a 4-fold higher dose, i.e. 4 µg/mL, for the same effect. The minimum inhibitory concentration of $^{Cu_2L}P_{60\%}$ was determined as low as 0.64µg/mL. Excellent stability of the poly(acrylate) microgels was observed by negative zeta potentials in nanopure water and aqueous sodium dodecyl sulfate solution. The composition of the microgel matrix with embedded binuclear metal complex was shown to be responsible for the antimicrobial activity, while the aqueous buffer-surfactant solution is not.

1. Introduction

Antimicrobial resistance is increasing worldwide at an alarming pace.[1] Growing numbers of bacteria evade currently available antibiotics rendering their continued use ineffective. In fact, the resistance of bacteria against currently available drugs is increasing faster than the development of new antimicrobial agents.[2] Approaches focusing on synthesizing new low molecular weight antibiotics are unfortunately likely to give similar results due to fast adaption and evolution of the targeted bacteria, with the potential to magnify rather than mitigate the problem. Along with a responsible use of currently available drugs, new strategies,[1, 3] compounds,[4] and compound classes are needed that are unlikely to trigger further expansion of bacterial resistance.[1] A promising strategy in this regard is the development of new antibiotic agents based on nanostructured surfaces,[5] block copolymer micelles,[6] gels,[3] and nanoparticles[3] for which the classic resistance mechanisms of bacteria are not evident at this time.[1, 4, 7] Among these, micro- and nanogels are particularly appealing as cross-linked gels are demonstrated to function as carriers for antimicrobial peptides,[8] hydrophilic drugs,[9] metal ions,[10] and low molecular weight antibiotics.[11-13]

In a previous study, we developed biomimetic microgel catalysts that show a remarkable ability to hydrolyze glycosidic bonds under physiological conditions surpassing the performance of catalytic antibodies.[14] The spherical, water-dispersed microgels (**Figure 1**) are synthesized from miniemulsions that are obtained by ultra-sheering of monomer mixtures in aqueous solutions.[15-18] A pre-polymerization mixture typically consists of ethyleneglycol dimethacrylate (EGDMA, **1**) as a crosslinking agent, butyl acrylate (BA, **2**) as a monomer, and VB(bpdpo) (**3**) as a pentadentate backbone ligand (**Chart 1**).[14]

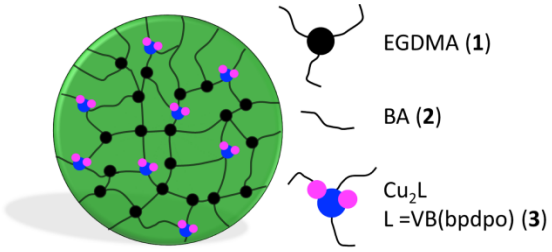

Figure 1. Schematic representation of the microgel architecture

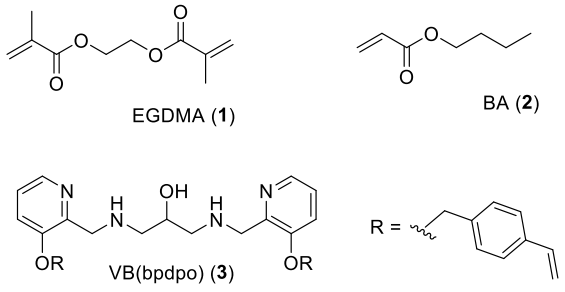

Chart 1. Structures of monomers in a typical microgel synthesis

The monomer mixtures yield stabilized droplets after ultra-sheering in presence of a hydrophobe in an aqueous buffer-surfactant solution. The subsequent polymerization captures these droplets without alteration of their size as micro- or nanogels.[17-18] The immobilized ligand is usually transformed *in-situ* into a binuclear metal complex by addition of copper(II) acetate prior to polymerization.[15, 19-20] To prevent interference of the paramagnetic copper(II) ions with the radical polymerization, mannose and other counter ions are added to

the pre-polymerization mixture in aqueous buffer-surfactant solutions.[15] The procedure saturates the metal complex core during material synthesis and prevents metal ion leakage and interference with the polymerization reaction. The resulting microgels have a size between 204 nm (5 % crosslinked) and 270 nm (80% crosslinked).[21]

When exploring the substrate scope of the developed microgel catalysts, a surprisingly efficient catalytic hydrolysis of 4-methylumbelliferyl *N*-acetyl-*β*-D-glucosaminide (**4**) was noted (**Chart 2**).[22] Model substrate **4** has the same amino sugar moiety and *β*-glycosidic linkage as *N*-acetylmuramic acid (**5**) and *N*-acetylglucosamine (**6**) (**Chart 2**), which are building blocks in the peptidoglycan layer of the bacterial cell wall of Gram-positive bacteria.[23] Intrigued by this observation, we exposed *Staphylococcus aureus* as a model for other Gram-positive bacteria to the developed polyacrylate microgels. The results of the study establish antimicrobial activity of the microgels with immobilized metal complex and demonstrate susceptibility of the bacteria to this class of antimicrobial agents. Details of the conducted structure-activity relationship study disclosing contributions of microgel composition, size, and zeta potential toward the observed minimum inhibitory concentration (MIC) and minimal bactericidal concentration (MBC) are discussed below.

2. Results and discussion

The antimicrobial activity of water-dispersed microgels against *Staphylococcus aureus* (ATCC® 25923™) is obtained using broth microdilution assays as outlined by the Clinical and Laboratory Standards Institute (CLSI).[24] In short, the minimum inhibitory concentration is determined for each microgel in 96-well plate assays. All assays are performed with *S. aureus* bacteria in their mid-exponential growth phase in Mueller Hinton broth with two independent inoculums at a final concentration of 2.5×10^5 CFU/mL each. The concentration of each bacterial suspension is determined immediately prior to use and adjusted to the absorbance reads of a 0.5 McFarland standard at 625 nm with broth medium to account for a concentration of the bacterial suspension of 1×10^8 CFU/mL.[24-26] Purity and growth controls are included on each plate. The microgels are used in nominal concentrations between 0.03 and 16 µg/mL that are based on the experimentally determined amounts of immobilized ligand (L = VBbpdpo (**3**)).[15] Due to slight turbidity apparent after addition of the microgel dispersions to the broth-containing wells, changes in absorbance are recorded for each well at 595 nm using UV/Vis spectroscopy over 18 to 24 h in 2 h time intervals. MIC values are determined for each microgel concentration by linear regression of the differences in absorbance reads recorded for the time of steady state of bacterial growth compared to time zero. Steady state of bacterial growth is typically reached after incubation of the plates for 8 to 12 hours.

Microgels with a crosslinking content between 5 ($^{Cu_2L}P_{5\%}$) and 80 mol % ($^{Cu_2L}P_{80\%}$) show MIC values between 0.93 and 0.64 µg/mL (**Table 1**, entries 1-5). Thus, the antimicrobial activity increases with the crosslinking content of the microgels and levels out when 60 mol% or more of EGDMA are used during material synthesis (**Figure 2**). All determined MIC values for the polymers are below the breakpoint of 2 µg/mL indicating susceptibility of the selected *S. aureus* strain to the microgels as antimicrobial agents.[24] To determine the building blocks in the modular synthesis of the microgels that cause the observed antimicrobial activity, a series of control experiments is conducted (**Table 1**, Entries 6-17, **Figure 3**). As all microgels are subject to 20 dialysis cycles for purification prior to use in antimicrobial assays, residual hydrophobes, salts, sugar counter ions, and unreacted monomers of the synthesis are thereby quantitatively removed. The resulting microgels contain 0.5 mol% of immobilized Cu(II) complex in an aqueous CAPS buffer solution with SDS surfactant.[14-15, 21-22, 27]

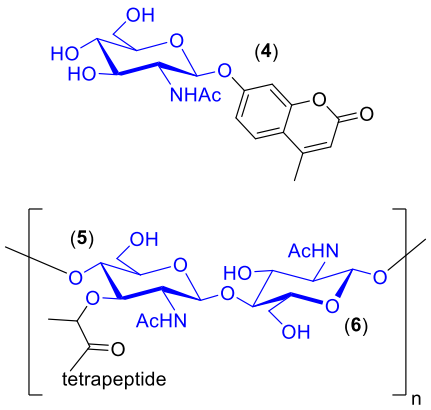

Chart 2. Structures of model substrate (**4**) and building blocks (**5**) and (**6**) of the peptidoglycan in cell walls of Gram-positive bacteria.

Table 1. Minimum inhibitory concentrations of microgels, control agents, and commercial low molecular weight antibiotics against *Staphylococcus aureus* (ATCC® 25923™).

Entry	Antimicrobial agent	MIC [µg/mL]
Microgels		
1	$^{Cu_2L}P_{5\%}$	0.93 ± 0.01
2	$^{Cu_2L}P_{25\%}$	0.72 ± 0.01
3	$^{Cu_2L}P_{40\%}$	0.68 ± 0.02
4	$^{Cu_2L}P_{60\%}$	0.64 ± 0.01
5	$^{Cu_2L}P_{80\%}$	0.64 ± 0.01
Controls		
6	$^{L}P_{60\%}$	0.67 ± 0.03
7	$^{S}P_{60\%}$	0.77 ± 0.02
8	Cu_2bpdpo	395 ± 5
9	$Cu(OAc)_2$	≥ 513
10	EGDMA (**1**)	≥ 270
11	BA (**2**)	≥ 80
12	SDS	122 ± 1
13	SDS/CAPS	128 ± 3
Commercial antibiotics		
14	Vancomycin (**7**)	2.4 ± 0.2
15	Benzalkonium chloride (**8**)	3.6 ± 0.2
16	Chloramphenicol (**9**)	6.1 ± 0.1
17	Sulfamethoxazole (**10**)	26.0 ± 0.5

Most notably, the microgel $^{Cu_2L}P_{60\%}$ (**Table 1**, Entry 4) shows a 617-fold higher antimicrobial activity than its low molecular weight analog, the binuclear copper(II) complex Cu_2bpdpo (**Table 1**, Entry 8). Based on the known stability constant of the complex ($K_a = 10^{17}$ M^{-2})[19] and the concentra-

tion of the immobilized VBbpdpo (**3**) ligand (8.75×10^{-4} M), a concentration of 0.013 µg/mL of free Cu(II) ions leaching from the complex was calculated. However, the MIC value of free Cu(II) ions is larger than 513 µg/mL (**Table 1**, Entry 9) indicating that free Cu(II) ions are not a likely source of the observed antimicrobial activity of the microgel $^{Cu}_{2}{}^{L}P_{60\%}$. Likewise, unreacted monomers that may have not been removed during the excessive dialysis cycles are not a source for antimicrobial activity of $^{Cu}_{2}{}^{L}P_{60\%}$ (**Table 1**, Entries 10 and 11). A comparison of the MIC value of $^{Cu}_{2}{}^{L}P_{60\%}$ to its metal ion-free analog $^{L}P_{60\%}$ (**Table 1**, Entry 6) indicates a small contribution of the copper(II) content to the overall observed activity of $^{Cu}_{2}{}^{L}P_{60\%}$. Similarly, the contribution of the immobilized ligand to the overall observed activity of $^{Cu}_{2}{}^{L}P_{60\%}$ is small, yet apparent when comparing microgels that contain equal amounts of VBbpdpo ($^{L}P_{60\%}$) and styrene ($^{S}P_{60\%}$) (**Table 1**, Entry 7). The antimicrobial activities of the aqueous SDS surfactant and CAPS/SDS solutions are rather low as well (**Table 1**, Entries 12 and 13) indicating that the observed antimicrobial ability of $^{Cu}_{2}{}^{L}P_{60\%}$ is due to the microgel itself and not due to the surfactant used during material synthesis. Our observations are in line with remarks of others that note antimicrobial activity of SDS solutions with concentrations above 100 µg/mL,[28] and above 3 wt%.[29] The MIC value of SDS solutions has been described as 1 mM (= 288 µg/mL),[30] which is even higher than the MIC value determined in our study. The selected strain of *S aureus* is thus already defined as resistant against the chosen surfactant by others. Nevertheless, SDS solutions of high concentrations are known to lyse the bacterial membranes, resulting in leakage of cytoplasmic components, and concomitant cell death.[30] Given this series of experimental evidence, we ascribe significant contributions of the observed antimicrobial activity of microgel $^{Cu}_{2}{}^{L}P_{60\%}$ to its polyacrylate matrix surrounding the immobilized metal complex. A similar effect was observed upon incorporation of vancomycin onto dextran nanoparticle surfaces,[31] albeit the improvement of the MIC value upon conjugation was only 2-fold when compared to the unconjugated agent (MIC = 1 µg/mL).

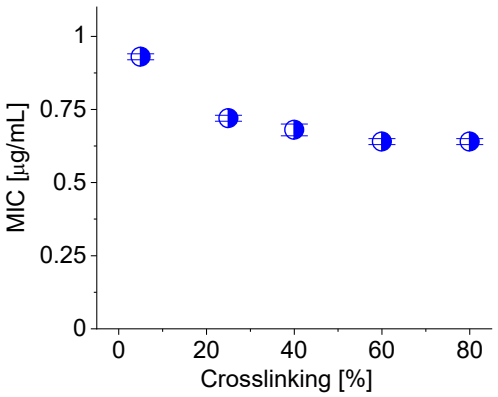

Figure 2. MIC values of microgels $^{Cu}_{2}{}^{L}P_{5\text{-}80\%}$ as a function of their crosslinking content.

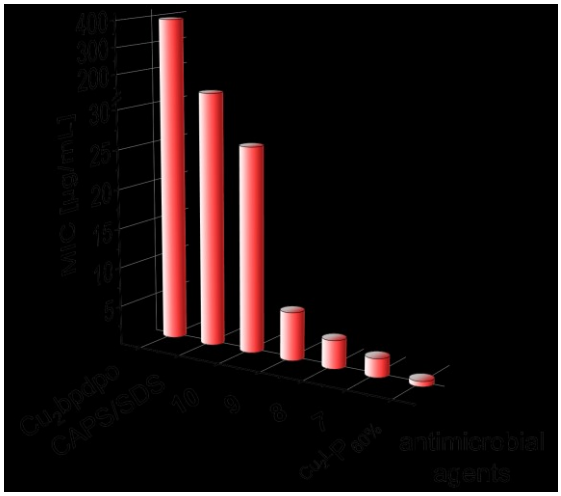

Figure 3. MIC values of microgel $^{Cu}_{2}{}^{L}P_{60\%}$ and control agents

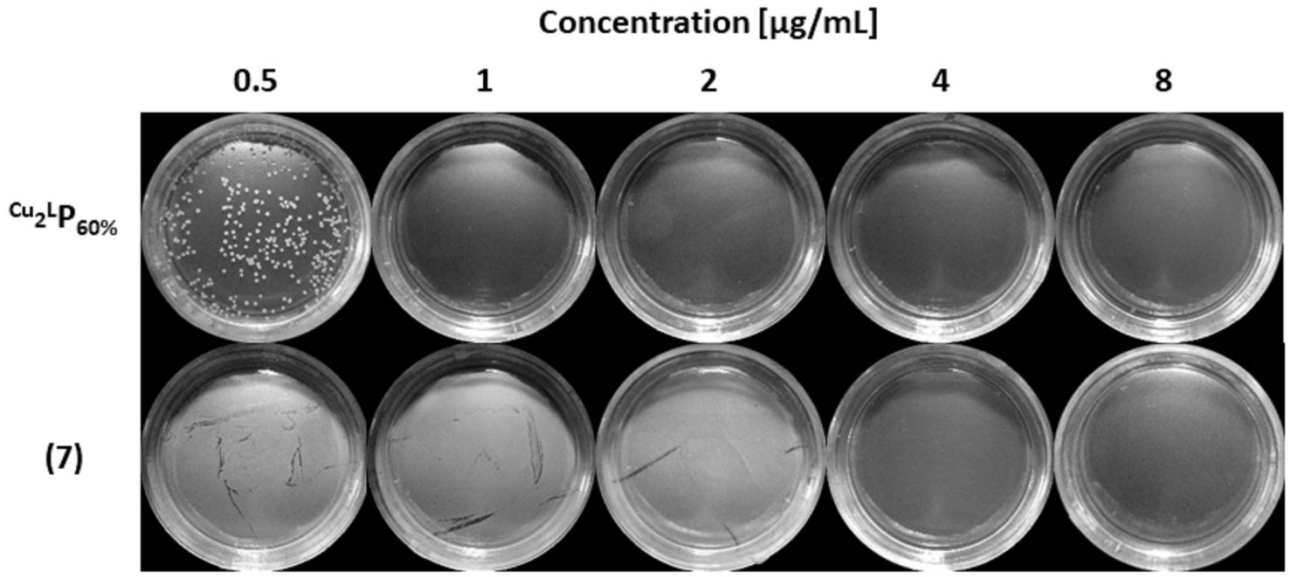

Figure 4. Growth of *S. aureus* after exposure to microgel $^{Cu}_{2}{}^{L}P_{60\%}$ and vancomycin (**7**) in Petri dishes (Ø 60 mm)

Other control experiments include assessments of common low molecular weight agents against the selected *S. aureus* strain with the developed assay. The observed antimicrobial activity (**Table 1**, Entries 14-17) is comparable to that described in the literature, i.e. MIC = 0.5-2 µg/mL for vancomycin (**7**),[32-35] 2-16 µg/mL for benzalkonium chloride (**8**),[36-39] 3.91-16 µg/mL for chloramphenicol (**9**),[40-41] and 25-32 µg/mL for sulfamethoxazole (**10**).[42-43] In our assay, the *S. aureus* strain is thus not susceptible, but intermediate and even resistant to these commercial agents, while it is susceptible to $^{Cu}{}_{2}{}^{L}P_{60\%}$ (**Figure 3**) and all other microgels (**Table 1**). This observation offers opportunities for the designed microgels as antimicrobial agents at occasions, where standard drugs fail to show the desired activity.

To highlight the antimicrobial activity of the microgels in comparison to the commercial agents further, their minimal bactericidal concentration is determined. The cell viability is observed after re-plating of cell suspensions after exposure to microgels and commercially available antimicrobial agents in different concentrations over 18 h. The MBC is determined from the observed cell growth and lack thereof after incubation for additional 24 h. Imaging the cell growth of bacterial suspensions after exposure to $^{Cu}{}_{2}{}^{L}P_{60\%}$ and vancomycin (**7**) at concentrations between 0.5 and 8 µg/mL reveals bactericidal activity of the microgel at 1 µg/mL, while the MBC of is 4 µg/mL (**Figure 4**). In more detail, the growth of separate *S. aureus* colonies is visible for a plate growing cells exposed to 0.5 µg/mL of $^{Cu}{}_{2}{}^{L}P_{60\%}$, while a lawn-like growth of the bacteria is observed for corresponding Petri dish plates with exposure to at 0.5, 1, and 2 µg/mL. The results indicate a 4-fold higher bactericidal activity of the microgel than for **7**. Subsequently, the exposure time of the microgel to the bacteria was shortened to 0, 1, 2, 4, 6, 10, 14, and 18 h using $^{Cu}{}_{2}{}^{L}P_{60\%}$ at its bactericidal concentration of 1 µg/mL in otherwise identical assays. To avoid antimicrobial carry-over, all aliquots taken from the bacteria suspensions are diluted by 1 : 50 with 0.9 % saline solution prior to plating. The apparent bacterial growth after 24 h of incubation at 37 °C indicates bactericidal activity of the microgel at this concentration after 1 h or less (see Supporting Information, **Figure S6**).

All other microgels show bactericidal activity comparable to $^{Cu}{}_{2}{}^{L}P_{60\%}$. SDS and SDS/CAPS solutions are bactericidal at 234 µg/mL indicating again that the observed activity is due to features of the microgel, and not due to the aqueous buffer-surfactant solution. Furthermore, benzalkonium chloride (**8**) is bactericidal at 4 µg/mL, chloramphenicol (**9**) at 512 µg/mL, and sulfamethoxazole (**10**) above 512 µg/mL. The low molecular weight complex Cu_2bpdpo remains bacteriostatic at 512 µg/mL indicating again contributions of the matrix to the overall observed antimicrobial activity of the microgels with embedded binuclear copper(II) complex.

Therefore, microgel $^{Cu}{}_{2}{}^{L}P_{60\%}$, its copper ion-free derivative $^{L}P_{60\%}$, and ligand-free analogs $^{S}P_{60\%}$, $P_{60\%}$, and $PETA_{30\%}$ were characterized in their hydrodynamic diameter and zeta-potential (**Table 2**). The latter microgel contains 30 mol% of crosslinking PETA (**11**) in place of 60 mol% of EGDMA in $P_{60\%}$ and was synthesized using previously developed protocols (**Chart 3**).[15] Due to the structure of the selected monomers, $P_{60\%}$ and $PETA_{30\%}$ have the same nominal degree of crosslinking, yet the microgels contain different amounts of linear chain-forming butyl acrylate (**2**).

The hydrodynamic diameter of the microgels is between 243 nm for $P_{60\%}$ and 275 nm for $PETA_{30\%}$. The particle distribution is monomodal and the dispersity moderate (**Figures S4-5**). Notably, the zeta potential of all microgels is strongly negative (-80 - -90 mV) in aqueous SDS solution indicating excellent stability of the colloidal particles. Similar observations are made by others for related microgels.[44-46] The stability of the colloids increases even further with immobilization of a ligand, of styrene, and after coordination of copper(II) ions, and extends to microgel dispersions in nanopure water as well (**Figure 5**). The observations suggest an increase of the electrical potential between Stern and diffusion layer around the particles due to these changes in the microgel composition that enhance their colloidal stability. The corresponding antimicrobial activity of the microgels is highest for $^{Cu}{}_{2}{}^{L}P_{60\%}$ (vide infra), although a correlation to its hydrodynamic diameter and zeta potential is not apparent.

Table 2. Size and zeta-potential of selected microgels

Entry	Microgel	D_h [nm]	ζ_{SDS} [mV]	ζ_{H2O} [mV]
1	$P_{60\%}$	243 ± 1	-80.3 ± 2.2	-63.4 ± 1.0
2	$^{Cu}{}_{2}{}^{L}P_{60\%}$	253 ± 3	-84.7 ± 2.0	-62.7 ± 1.4
3	$^{L}P_{60\%}$	253 ± 3	-85.3 ± 0.5	-62.6 ± 1.2
4	$^{S}P_{60\%}$	261 ± 5	-88.4 ± 2.7	-64.0 ± 1.6
5	$PETA_{30\%}$	275 ± 7	-89.7 ± 1.5	-69.3 ± 0.5

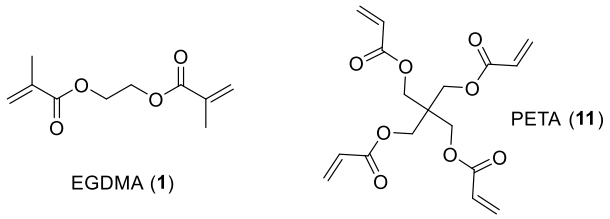

Chart 3. Structures of EGDMA (**1**) and PETA (**11**)

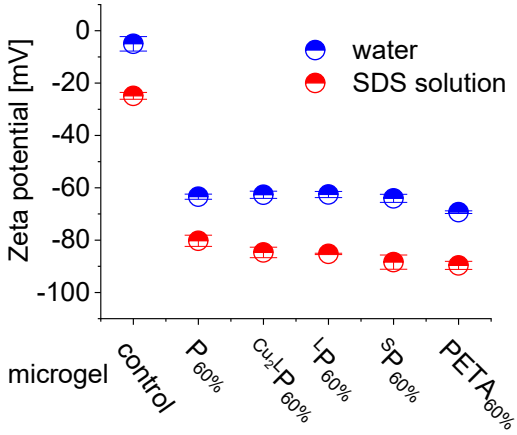

Figure 5. Zeta potential for microgel $^{Cu}{}_{2}{}^{L}P_{60\%}$ and derivatives

The minimum inhibitory concentration of the control microgels without immobilized additives is slightly smaller for $PETA_{30\%}$ (41 ± 1µg/mL) than for $P_{60\%}$ (47 ± 2µg/mL) and determined relative to the dry weight of the respective microgels. The results imply that poly(acrylate)s derived from crosslinking PETA support similar, and maybe stronger, interactions with bacteria than EGDMA due to the altered morphology of the resulting microgels. Additionally, the lower amount of crosslinker for microgels derived from PETA allows the

incorporation of a larger amount of other functional monomers and thereby further tuning of material properties.

In order to obtain preliminary data for the cytotoxicity of the developed microgels, THP-1 cells and the microgel $^{Cu}_{2}{}^{L}P_{60\%}$ were used in subsequent efforts.[47-50] In a typical experiment, monocytes were grown in RPMI-1640 medium to a density of 1×10^6 cells/mL. Twelve aliquots of these cells were exposed to $^{Cu}_{2}{}^{L}P_{60\%}$ at its minimal inhibitory concentration over 1 h in humid 5 % CO_2 atmosphere prior to addition of resazurin blue dye and continued incubation over 4 additional hours. The viability of the cells was determined by reads of fluorescence intensity ($8.51 \pm 0.3 \times 10^6$) and compared to data for cells treated similarly in absence of microgel ($8.53 \pm 0.2 \times 10^6$). The comparison reveals viability of more than 99 % of THP-1 cells implying low cytotoxicity of the microgels towards this cell line under the given conditions. In-depth studies are topic of on-going investigation and will be reported soon.

Conclusions

The structure-activity relationship study establishes water-dispersed microgels with immobilized metal complex as promising new class of antimicrobial agents that surpass several commercially available drugs in their activity. *S. aureus* is susceptible to the polyacrylate microgels, but found intermediate and resistant to common low molecular weight antibiotics. The microgel $^{Cu}_{2}{}^{L}P_{60\%}$ is nontoxic at its minimal inhibitory concentration to human THP-1 cells and bactericidal to S. aureus at 1 μg/mL, while the minimal bactericidal concentration of vancomycin (**7**) is 4-fold higher, i.e. at 4 μg/mL. Control experiments reveal a 617-fold increase of antimicrobial activity when comparing a low molecular weight binuclear copper(II) complex Cu_2L to its microgel analog $^{Cu}_{2}{}^{L}P_{60\%}$. Variations in the crosslinking content of the microgel matrix between 5 and 80 mol% reveal optimized activity of 0.64 μg/mL at 60 mol% of crosslinking. A systematic removal of copper(II) ions and of ligand emphasizes the contributions of the immobilized complex to the apparent activity. All microgels have a strongly negative zeta potential in aqueous SDS solution and in nanopure water indicating excellent stability of the formed particles. Lastly, a series of control experiments indicates an opportunity to design poly(acrylate) microgels from crosslinking PETA with the altered morphology and improved antimicrobial activity in future efforts for further development of these promising new antimicrobial agents.

3. Experimental details

3.1 Instrumentation

A Digital Sonifier (Branson) with flat cap was used for ultrasonication. A medium- pressure lamp TQ 150 (Heraeus Noblelight) with a current of 2.0 A, a voltage of 90 V, and an outer diameter of 13.50 mm was used for free radical polymerizations. Nanopure water at a resistance of 18.2 MΩ was obtained from a Barnstead E-PureTM ultrapure water purification system (ThermoScientific). Polymer aliquots were air-dried using an IKA Dry Block Heater (VWR). Elemental analyses of the microgels were obtained from Atlantic Microlab, Atlanta, GA. Hydrodynamic diameters and zeta potentials were obtained on a Zetasizer NanoZS with NanoSampler (Malvern Panalytical) equipped with a He-Ne laser at a wavelength of 632.8 nm. All data were acquired and analyzed using the supplied Zetasizer Software, version 7.13. UV/Vis absorbances were obtained on a Cary 50 UV/Vis spectrometer (Varian) equipped with WinUV Analysis Suite software, version 3.0. Bacterial and THP-1 growth was observed on a FilterMax F5 Multi-Mode Microplate Reader (Molecular Devices) equipped with SoftMax Pro 6 software, version 6.3. Solutions, growth media, and pipet tips were sterilized using a Sterilmatic Steam Pressure Autoclave (Market Forge) operated at 121 °C and 15 psi for 35 min; bacteria were grown using an incubating Mini Shaker (VWR) operated at 240 rpm and 37 °C. All bacterial suspensions were handled in a Delta Series Class II Type A2 Biosafety Cabinet (Labconco). THP-1 cell suspensions were grown in a Heracell™ VIOS 160i CO_2 Incubator (Thermo Scientific), and handled in a LabGard NU-407FM-400 Laminar Flow Biosafety Cabinet (NuAire).

3.2 Materials

Spectra/Por membranes (Spectrum Laboratories) with a molecular weight cutoff (MWCO) of 15,000 were used for dialysis. All pH values were measured after three-point calibration using a Φ 250 pH meter (Beckman) equipped with a refillable combination pH electrode (ROSS Orion). The electrode had a 165 mm long epoxy body and a 95 mm long semi-micro tip with a diameter of 8 mm. Bottle-top filters (Nalgene) with 500 mL volume, 0.22 μm pore size and polyethersulfone (PES) membrane were used for filtration of aqueous buffer and SDS solutions. Zeta potentials were measured in Folded Capillary Zeta Cells (Malvern Panalytical); a quartz flow cell (Malvern Panalytical) was used to measure hydrodynamic diameter; 15 and 50 ml sterile clear polypropylene centrifuge tubes with conical bottom (VWR) were used for bacterial growth; disposable polycyclical olefin 2.5 mL macro cells with 10 mm pathlength (BrandTech) were using when adjusting the bacterial count to a 0.5 McFarland standard; Acrodisc® sterile syringe filter with 0.2 μm Supor Membrane® (Pall Laboratory) were used for sterilization of the metal complex solutions; clear, medium binding, flat-bottom, chimney 96-well microlon ELISA-plates (Greiner Bio-One) were used for the determination of minimum inhibitory concentration of antimicrobial agents; clear flat-bottom, medium-binding, chimney 96-well black polystyrene microplates (Greiner Bio-One) were used for cell viability assays; heat-resistant polyester films (VWR) were used as adhesives for 96-well plates; a hemocytometer with improved Neubauer Bright-Line™ grid and 0.1 mm depth (American Optical) was used for manual cell count; and sterile, disposable round polystyrene Petri dishes, 15 × 60 mm, (VWR) were used for the determination of the minimal bactericidal concentration of antimicrobial agents.

3.3 Chemicals.

Sodium dodecyl sulfate (SDS), styrene, sulfamethoxazole (**10**), and pentaerythritol tetraacrylate (PETA, **11**) were purchased from TCI America; ethylenediaminetetraacetic acid disodium salt, decane, 2,2'-dimethoxy-2-phenylacetophenone, copper(II) acetate monohydrate, sodium hydroxide, pyrocatechol, and *N*-cyclohexyl-3-aminopropanesulfonic acid (CAPS), agar, a sterile Fetal Bovine Serum (FBS) solution, and a sterile-filtered antimycotic solution with 10,000 units of penicillin, 10 mg streptomycin and 25 μg amphotericin B per mL from Sigma-Aldrich; ethylene glycol dimethacrylate (EGDMA, **1**) and barium chloride dihydrate from Alfa Aesar; butyl acrylate (BA, **2**) and neutral aluminum oxide from Acros Organics; methanol from EMD Millipore; Sulfuric acid and sodium chloride from VWR Chemicals BDH®; Ethanol from Koptec; benzalkonium chloride (**8**) from BeanTown Chemical; chloramphenicol (**9**) from IBI Scientific; vancomycin hydrochloride (**7**) from VWR Life Science; Mueller Hinton broth base from Hardy Diagnostics; *Staphylococcus aureus*

(ATCC® 25923™); and Roswell Park Memorial Institute medium (RPMI-1640) from the American Type Culture Collection; Trypan Blue solution for cell staining from GE Healthcare Life Science and a Deep Blue Cell Viability™ Kit from BioLegend. THP-1 cells were obtained as a generous gift from Steven C. Woods at the U. S. Food and Drug Administration, Silver Spring, MD. All other chemicals had reagent grade or higher, were stored as instructed by the manufacturer, and used as received unless noted otherwise.

EGDMA (**1**), BA (**2**), and styrene were purified by filtration over neutral alumina immediately prior to use; A 2 mL aliquot of PETA (**11**) was purified by extraction with equal volumes of 10 % aqueous sodium hydroxide solution (3x times) and nanopure water (3x times). For phase separation, each extraction was followed by 10 min of centrifugation at 6000 rpm. The organic layer was dried with sodium sulfate, centrifuged, and used as is. The polymerizable ligand *N*,*N*'-bis-((3-(4-vinylbenzyloxy)-2-pyridylmethyl)-1,3-diaminopropan-2-ol (VBbpdpo, **3**),[51] microgels $^{Cu}{}_{2}{}^{L}P_{5\text{-}80\%}$,[15] and the low molecular weight complex *N*,*N*'-[bis(2-pyridylmethyl)-1,3-diaminopropan-2-ol]ato dicopper(II) (μ-acetato) diperchlorate, Cu_2bpdpo,[52] were synthesized as described.

3.4 Microgel synthesis and characterization

The strategy for the synthesis and characterization of microgels with VBbpdpo ligand, $^{Cu}{}_{2}{}^{L}P_{5\text{-}80\%}$, was discussed in detail previously.[15] Thus, only experimental details for the synthesis and characterization of the microgels $^{S}P_{60\%}$, $P_{60\%}$, and $PETA_{30\%}$ are given here.

3.4.1 Microgel $^{S}P_{60\%}$.

In a typical experiment, a mixture of 0.8343 g (4.209 mmol) EGDMA (**1**), 0.3613 g (2.819 mmol) BA (**2**) and 0.0212 g (0.2036 mmol) styrene was prepared. Three aliquots of 0.3028-0.3043g monomer mixture were suspended in 9.6016-9.6036g 52 mM SDS solution with 0.0801-0.0815g decane each.

The suspensions were cooled in ice, sonicated, and polymerized under UV light after initiation with 10 mol% of 2,2-dimethoxy-2-phenylacetophenone in the cold as described.[15] Of the three reaction vessels, one was left undisturbed for 60 min. Aliquots of the reaction mixtures were taken from the other two in regular time intervals over 75 min and treated with pyrocatechol to inhibit further polymerization.[15] The aliquots were dried at 60°C to constant weight to determine their solid content. The degree of polymerization was determined after correction of solid content from the SDS solution to 94% at 60 min (see Supporting Information, **Figure S1**).[15]

The dry weight of microgel per volume was determined as 32.9 mg/ml by drying two aliquots of microgel suspension and correcting for the weight of SDS before averaging. The weight of SDS in the microgel aliquot was determined by drying a corresponding aliquot of aqueous SDS solution. The amount of styrene was determined as 500 µg/ml of microgel suspension from the amount of styrene in the pre-polymerization mixture and the degree of polymerization assuming equal polymerization of all monomers. For determination of combustion data, a 1000µL aliquot of the microgel dispersion was dialyzed against water 20 times with 1 h intervals, and dried on aluminum pans at 60 °C for 48 h; calcd for $^{S}P_{60\%}$ C, 62.63; H, 7.76; found C, 61.33; H, 7.59.

3.4.2 Microgel $P_{60\%}$

In a typical experiment, the microgel was synthesized from a mixture of 0.3389g (4.207 mmol) of EGDMA and 0.3604 g (2.812 mmol) of BA. After 60 min, the degree of polymerization is 98% and the dry weight of the polymer is 31.3 mg/mL. Calcd for $P_{60\%}$ C, 62.10; H, 7.76; found C, 61.57; H, 7.57; see Supporting Information, **Figure S2**)

3.4.3 Microgel $PETA_{30\%}$.

In a typical experiment, the microgel was synthesized from a mixture of 0.7486 g (2.125 mmol) of PETA and 0.6290 g (5.415 mmol) of BA as described above. The degree of polymerization is 94 % at 60 min. The dry weight of the polymer is 33.8 mg/ml in the microgel suspension at the same time. Calcd for $PETA_{30\%}$ C, 61.63; H, 7.45; found C, 61.12; H, 7.13. (see Supporting Information, **Figure S3**)

3.5 General procedure for pre-treatment of microgels for characterization by size, zeta potential, and antimicrobial activity

Typically, 200 µL aliquots of three microgels are dialyzed against 80 mL of aqueous 0.46 mM $EDTANa_2$/ 52 mM SDS solution (5x) with 2 h intervals, then 80 mL each of 52 mM aqueous SDS solution (15x) with 1 h intervals, and finally against 80 mL of 50 mM CAPS/52 mM SDS solution (4x) with 2 h intervals. The microgel dispersions are then diluted into 2 mL with the same aqueous CAPS/SDS solution.

For measurements of hydrodynamic diameters, a 200 µL aliquot of this stock solution is diluted into 5 mL with 52 mM SDS solution; 1 mL of the resulting solution is further diluted into 5 mL. The resulting solution is stored at ambient temperature, and used as is.

For measurements of zeta potentials, the 200 µL aliquot is treated likewise, but diluted with nanopure water. For all microgels that do not contain VBbpdpo ligand, CAPS-free solutions are used for dialysis and dilutions.

For determination of antimicrobial activity, microgels with VBbpdpo ligand are treated with appropriate volumes of 14 mM Cu(II) acetate solution after dialysis to reach complete ligand saturation prior to dilution of a 400 µL aliquot of the stock solution into 2 mL with aqueous 52 mM SDS/50 mM CAPS solution. The ligand concentration of the resulting microgels dispersions is typically 0.10-0.15 mM or 64-90 µg/mL, the dry weight of the microgels is 6.0-6.5 mg/mL.

3.5.1 Determination of microgel size

Hydrodynamic diameters were obtained using a measuring angle of 173° for back scattering of the samples at 20 °C after an equilibration time of 120 s before the first measurement. The data were recorded for settings of the material as a polystyrene latex with a refractive index of 1.590, an absorption of 0.010, and nanopure water as the dispersant. Each sample was measured in triplicate as an average of 10 accumulations each over 10 s duration without delay between measurements. The reported hydrodynamic diameters are given as an average of the resulting data.

3.5.2 Determination of microgel zeta potential

Zeta potential data were obtained for samples at 20 °C after an equilibration time of 120 s before the first measurement. The data were recorded for settings identical to those described above. Each sample was measured in triplicate as an average of 20 accumulations without delay between measurements. The reported zeta potentials are given as an average of the acquired data.

3.6 Broth microdilution assays

Following the guidelines from the Clinical and Laboratory Standards Institute,[24] sterile Mueller Hinton (MH) broth, Mueller Hinton agar plates, and a 0.5 McFarland standard were prepared (see Supporting Information).[25-26, 33] The purchased bacterial *S. aureus* slab (ATCC® 25923™) was transferred into culture starters in Muller-Hinton medium as recommended by the manufacturer. Typically, 500 µL aliquots of these starter cultures are flash frozen in liquid nitrogen and stored at -20 °C until use.

3.6.1 Bacteria growth

In a typical experiment, culture starters of *S. aureus* are thawed and propagated with shaking in 5 mL Mueller-Hinton both at 37 °C. After 5 h, a 500 µL aliquot of the inoculum is serially diluted into Mueller-Hinton broth (500µL→20mL; 1→10mL; 1→10mL; 1→10mL). Subsequently, a 50 µL aliquot of the diluted bacteria suspension is plated on Mueller-Hinton agar in Petri dishes and incubated at 37 °C.

After 24h, 7-10 well-isolated colonies are re-suspended in 4 mL of Mueller-Hinton broth. About 3 mL of this suspension are transferred into a UV/Vis cuvette and matched by optical density reads at 625 nm and 37°C to a 0.5 McFarland standard by further broth addition. The nominal bacterial concentration of the resulting suspension is 1×10^8 CFU/mL. Finally, a 50 µL aliquot of the standardized bacterial suspension is diluted volumetrically into 10 mL with Mueller Hinton broth to a nominal concentration of 5×10^5 CFU/mL of *S. aureus* and used. Typically, two independent bacteria cultures are grown in parallel.

3.6.2 Microgel preparation

In a typical experiment, 754 µL of microgel $^{Cu}{}_2{}^{L}P_{60\%}$ that is 84.9 µg/mL in ligand concentration (see 3.5 above) are diluted into 1 mL volumetrically with Mueller-Hinton broth yielding a microgel dispersion that is 64 µg/mL in ligand concentration. The microgel dispersion is steam-sterilized, cooled, and stored at ambient temperature until use. All other microgels are treated likewise (see Supporting Information).

3.6.3 Assay preparation

With each of the independent bacteria cultures, four antimicrobial agents are evaluated in one 96-well plate assay. Initially, all wells are filled with 100 µL of Mueller Hinton broth. Then, 100 µL aliquots of selected antimicrobial agents are added to the first column to the left on the plate in landscape orientation and mixed. A 100 µL aliquot of the mixture is transferred to the right and treated likewise until reaching column 10. The 100 µL aliquot of column 10 is not transferred to column 11, but disposed. Finally, 100 µL aliquots of the bacterial stock solution are added to the first column to the left and treated likewise until column 10. A 100 µL aliquot of bacteria is added to column 11 as a growth control, while column 12 contains broth only and functions as purity control in the assay. The nominal concentration of each well containing bacteria is 2.5×10^5 CFU/mL. Typical concentrations of the antimicrobial agent range between 0.03 and 16 µg/mL.

3.6.3 Data collection

The prepared 96-well plate was sealed with an adhesive heat-resistant film, exposed to orbital shaking for 2 min, and incubated at 37 °C. The bacterial growth was monitored by absorbance reads after additional 30 s orbital shaking at 595 nm over a time period of 18-24 h in 2 h intervals.

3.6.4 Data analysis

All incubated 96-well plates with evidence for bacteria in the purity control columns were disposed and not analyzed. Due to the slight turbidity of the microgel suspensions in the Mueller Hinton broth, analysis of bacterial growth on the plates by naked eyes is limited and used as an estimate. In addition, the recorded absorbance reads were analyzed by linear regression.

Along these lines, recorded absorbance data for steady state of bacteria growth are corrected for initial absorbance of the mixtures at time zero and plotted against the concentration of the selected antimicrobial agent. A linear fit (y=ax+b) was applied to the resulting data, and the minimum inhibitory concentration deduced at y=0. Data were not considered for analysis, when the difference in absorbance reads ΔA_{595} is 0.05 or less. MIC values are given as an average of two or more independent experiments.

3.7 Assay to determine minimal bactericidal concentrations

Typically, 50 µL aliquots of three or more cell cultures exposed to different concentrations of the antimicrobial agent in broth microdilution assays were spread over separate Mueller-Hinton agar plates and incubated at 37 °C. After 24 h, the plates were examined for bacterial growth with the naked eye and imaged. The minimal bactericidal concentration of an antimicrobial agent was assigned to the lowest concentration that inhibits regrowth of bacteria.

3.8 Assay to estimate the required exposure time for bactericidal activity

The experimental set-up in 96 well-plates and the nominal bacterial concentration are identical to the conditions described for assays to determine the minimal bactericidal concentrations. In a typical experiment, 50 µL aliquots of cell cultures exposed to $^{Cu}{}_2{}^{L}P_{60\%}$ at 1 µg/mL for 0, 1, 2, 4, 6, 10, 14, and 18 h were diluted with 0.9 wt% saline solution and spread over separate Mueller-Hinton agar plates. After 24 h of incubation at 37 °C, the plates are examined for bacterial growth with the naked eye and imaged. The minimal exposure time for antimicrobial activity of $^{Cu}{}_2{}^{L}P_{60\%}$ is then deduced from the plate inhibiting regrowth of bacteria.

3.9 Cytotoxicity assay

3.9.1 Cell growth

THP-1 monocytes were grown in 40 mL suspensions over 4 days at 37 °C in a humid atmosphere containing 5% of CO_2 in a medium consisting of 89 % (v/v) of RPMI-1640, 10 % (v/v) of FBS, and 1 % (v/v) of an antibiotic antimycotic solution. Immediately prior to use, the cells were centrifuged at 1200 RPM (337 × RCF) for 10 min to replace the supernatant by equal volumes of new medium. Using a manual hemocytometer, a typical count of 1×10^6 cells/mL is observed in a suspension containing equal volumes of cell culture and trypan blue solution.

3.9.2 Microgel preparation

In a typical experiment, 755 µL of microgel $^{Cu}{}_2{}^{L}P_{60\%}$ that is 84.9 µg/mL in ligand concentration (see 3.5 above) are diluted into 5 mL with nanopure water volumetrically yielding a microgel dispersion that is 12.8 µg/mL in ligand concentration. The dispersion is steam-sterilized, cooled, and stored at ambient temperature until use.

3.9.3 Assay preparation.

In a 96-well plate assay, 10 µL of microgel suspension are added to 12 aliquots of 190 µL of cell culture each. After 1 h of incubation under cell growth conditions, 20 µL (10 volume %) of resazurin fluorescent dye are added, and the incubation continued for additional 4h. For a control experiment, the cell growth was observed in a likewise-prepared assay while substituting the microgel suspension by medium.

3.9.4 Data collection and analysis

The fluorescence of the added dye marks the viability of the cells and was recorded as intensity in arbitrary units at 595 nm (excitation at λ_{max} = 535 nm) and 37 °C after 10 min of equilibration as endpoint read with an integration time of 400 ms from the bottom of the plate. The obtained data were averaged for all 12 aliquots per experiment. The cell viability was deduced as percent value from a comparison of averaged intensity data for microgel-containing and microgel-free experiments. The data are given as an average of two independent sets of experiments.

ASSOCIATED CONTENT

Supporting Information. Gravimetric analyses of microgel formation for poly(acrylate)s without N-containing ligand, plots of intensity versus size, experimental details for preparation of stock solutions for microbroth dilution assays, and time-dependent images for bactericidal activity of $^{Cu}{}_2{}^{L}P_{60\%}$. This material is available free of charge via the Internet at http://pubs.acs.org.

AUTHOR INFORMATION

Corresponding Author

*E-mail: Susanne.striegler@uark.edu; phone: +1-479-575-5079 ; fax: +1-479-575-4049.

ORCID

Babloo Sharma: 0000-0002-0265-322X
Carlie M. Clem: 0000-0002-6600-0359
Alda Perez Diaz: 0000-0002-8376-8810
Susanne Striegler: 0000-0002-2233-3784

Author Contributions

The manuscript was written through contributions of all authors. All authors have given approval to the final version of the manuscript. ‡ B.S. and C.C. contributed equally to this work.

Notes

The authors declare no competing financial interests.

ACKNOWLEDGMENT

Support of this research to S.S. from the National Science Foundation (CHE-1854304) for the development of the microgels, and research grants from the Arkansas Biosciences Institute and the Chancellor's Commercialization Fund at the University of Arkansas for the development of antimicrobial assays are gratefully acknowledged. The THP-1 cells used in this study were a generous gift from Steven C. Woods at the U. S. Food and Drug Administration, Silver Spring, MD.

ABBREVIATIONS

ATCC, American Type Culture Collection; CFU, colony-forming units; CLSI, Clinical and Laboratory Standards Institute; D_h, hydrodynamic diameter; MBC, minimal bactericidal concentration; MH, Mueller-Hinton; MIC, minimum inhibitory concentration; MWCO, molecular weight cutoff; PDI, polydispersity index.

REFERENCES

1. Ganewatta, M. S.; Tang, C. Controlling macromolecular structures towards effective antimicrobial polymers. *Polymer* **2015**, 63, A1-A29.
2. Schaberle, T. F.; Hack, I. M. Overcoming the current deadlock in antibiotic research. *Trends Microbiol.* **2014**, 22, 165-167.
3. Muñoz-Bonilla, A.; Fernández-García, M. Polymeric materials with antimicrobial activity. *Prog. Polym. Sci.* **2012**, 37, 281-339.
4. Schulz, M.; Olubummo, A.; Binder, W. H. Beyond the lipid-bilayer: interaction of polymers and nanoparticles with membranes. *Soft Matter* **2012**, 8, 4849-4864.
5. Rigo, S.; Hürlimann, D.; Marot, L.; Malmsten, M.; Meier, W.; Palivan, C. G. Decorating Nanostructured Surfaces with Antimicrobial Peptides to Efficiently Fight Bacteria. *ACS Appl. Bio Mater.* **2020**, 3, 1533-1543.
6. Hisey, B.; Ragogna, P. J.; Gillies, E. R. Phosphonium-Functionalized Polymer Micelles with Intrinsic Antibacterial Activity. *Biomacromolecules* **2017**, 18, 914-923.
7. Echeverría, C.; Aragón-Gutiérrez, A.; Fernández-García, M.; Muñoz-Bonilla, A.; López, D. Thermoresponsive Poly(N-Isopropylacrylamide-co-Dimethylaminoethyl Methacrylate) Microgel Aqueous Dispersions with Potential Antimicrobial Properties. *Polymers* **2019**, 11, 606.
8. Nyström, L.; Al-Rammahi, N.; Malekkhaiat Häffner, S.; Strömstedt, A. A.; Browning, K. L.; Malmsten, M. Avidin–Biotin Cross-Linked Microgel Multilayers as Carriers for Antimicrobial Peptides. *Biomacromolecules* **2018**, 19, 4691-4702.
9. Michel, S. E. S.; Dutertre, F.; Denbow, M. L.; Galan, M. C.; Briscoe, W. H. Facile Synthesis of Chitosan-Based Hydrogels and Microgels through Thiol–Ene Photoclick Cross-Linking. *ACS Appl. Bio Mater.* **2019**, 2, 3257-3268.
10. Malzahn, K.; Jamieson, W. D.; Dröge, M.; Mailänder, V.; Jenkins, A. T. A.; Weiss, C. K.; Landfester, K. Advanced dextran based nanogels for fighting Staphylococcus aureus infections by sustained zinc release. *J. Mater. Chem. B* **2014**, 2, 2175-2183.
11. Xiong, M.-H.; Bao, Y.; Yang, X.-Z.; Wang, Y.-C.; Sun, B.; Wang, J. Lipase-Sensitive Polymeric Triple-Layered Nanogel for "On-Demand" Drug Delivery. *J. Am. Chem. Soc.* **2012**, 134, 4355-4362.
12. Lv, J.; Li, X.; Yin, H.; Wang, L.; Pei, Y.; Lv, X. Controlled release of vancomycin hydrochloride from a composite structure of polymeric films and porous fibers on implants. *Chem. Eng. J.* **2017**, 325, 601-610.
13. Michailidou, G.; Christodoulou, E.; Nanaki, S.; Barmpalexis, P.; Karavas, E.; Vergkizi-Nikolakaki, S.; Bikiaris, D. N. Super-hydrophilic and high strength polymeric foam dressings of modified chitosan blends for topical wound delivery of chloramphenicol. *Carbohydr. Polym.* **2019**, 208, 1-13.
14. Sharma, B.; Pickens, J. B.; Striegler, S.; Barnett, J. D. Biomimetic Glycoside Hydrolysis by a Microgel Templated with a Competitive Glycosidase Inhibitor. *ACS Catal.* **2018**, 8, 8788–8795.
15. Sharma, B.; Striegler, S. Crosslinked Microgels as Platform for Hydrolytic Catalysts. *Biomacromolecules* **2018**, 19, 1164–1174.
16. Utama, R. H.; Jiang, Y.; Zetterlund, P. B.; Stenzel, M. H. Biocompatible Glycopolymer Nanocapsules via Inverse Miniemulsion Periphery RAFT Polymerization for the Delivery of Gemcitabine. *Biomacromolecules* **2015**, 16, 2144-2156.
17. Antonietti, M.; Landfester, K. Polyreactions in miniemulsions. *Prog. Polym. Sci.* **2002**, 27, 689-757.
18. Landfester, K. Miniemulsion Polymerization and the Structure of Polymer and Hybrid Nanoparticles. *Angew. Chem., Int. Ed.* **2009**, 48, 4488-4507.
19. Striegler, S.; Dittel, M.; Kanso, R.; Alonso, N. A.; Duin, E. C. Hydrolysis of Glycosides with Microgel Catalysts. *Inorg. Chem.* **2011**, 50, 8869-8878.
20. Striegler, S.; Pickens, J. B. Discrimination of chiral copper(II) complexes upon binding of galactonoamidine ligands. *Dalton Trans.* **2016**, 45, 15203-15210.

21. Sharma, B.; Striegler, S.; Whaley, M. Modulating the Catalytic Performance of an Immobilized Catalyst with Matrix Effects - A Critical Evaluation. *ACS Catal.* **2018**, 8, 7710-7718.

22. Sharma, B.; Striegler, S. Nonionic surfactant blends to control the size and catalytic performance of microgels. *ACS Catal.* **2020**, 10, 9458–9463.

23. Vollmer, W.; Blanot, D.; de Pedro, M. A. Peptidoglycan structure and architecture. *Fems Microbiol. Rev.* **2008**, 32, 149-167.

24. CLSI, Methods for dilution antimicrobial susceptibility tests for bacteria that grow aerobically. In *Approved Standard—Tenth Edition*, Clinical and Laboratory Standards Institute: Wayne, PA, 2015.

25. Thattaruparambil Raveendran, N.; Mohandas, A.; Ramachandran Menon, R.; Somasekharan Menon, A.; Biswas, R.; Jayakumar, R. Ciprofloxacin- and Fluconazole-Containing Fibrin-Nanoparticle-Incorporated Chitosan Bandages for the Treatment of Polymicrobial Wound Infections. *ACS Appl. Bio Mater.* **2019**, 2, 243-254.

26. Contreras, A.; Raxworthy, M. J.; Wood, S.; Schiffman, J. D.; Tronci, G. Photodynamically Active Electrospun Fibers for Antibiotic-Free Infection Control. *ACS Appl. Bio Mater.* **2019**, 2, 4258-4270.

27. Sharma, B.; Striegler, S. Tailored Interactions of the Secondary Coordination Sphere Enhance the Hydrolytic Activity of Cross-Linked Microgels. *ACS Catal.* **2019**, 9, 1686-1691.

28. Kabara, J. J.; Swieczkowski, D. M.; Truant, J. P.; Conley, A. J. Fatty acids and derivatives as antimicrobial agents. *Antimicrob. Agents Chemother.* **1972**, 2, 23-28.

29. Garay-Jimenez, J. C.; Gergeres, D.; Young, A.; Lim, D. V.; Turos, E. Physical properties and biological activity of poly(butyl acrylate-styrene) nanoparticle emulsions prepared with conventional and polymerizable surfactants. *Nanomed.-Nanotechnol.* **2009**, 5, 443-451.

30. Yoon, B. K.; Jackman, J. A.; Kim, M. C.; Cho, N. J. Spectrum of Membrane Morphological Responses to Antibacterial Fatty Acids and Related Surfactants. *Langmuir* **2015**, 31, 10223-10232.

31. Hassan, M. M.; Ranzoni, A.; Phetsang, W.; Blaskovich, M. A. T.; Cooper, M. A. Surface Ligand Density of Antibiotic-Nanoparticle Conjugates Enhances Target Avidity and Membrane Permeabilization of Vancomycin-Resistant Bacteria. *Bioconjugate Chem.* **2017**, 28, 353-361.

32. Andrews, J. M. Determination of minimum inhibitory concentrations. *J. Antimicrob. Chemother.* **2001**, 48, 5-16.

33. Mauro, N.; Schillaci, D.; Varvara, P.; Cusimano, M. G.; Geraci, D. M.; Giuffre, M.; Cavallaro, G.; Maida, C. M.; Giammona, G. Branched High Molecular Weight Glycopolypeptide With Broad-Spectrum Antimicrobial Activity for the Treatment of Biofilm Related Infections. *ACS Appl. Mater. Interfaces* **2018**, 10, 318-331.

34. Hanberger, H.; Nilsson, L. E.; Maller, R.; Isaksson, B. Pharmacodynamics of daptomycin and vancomycin on Enterococcus faecalis and Staphylococcus aureus demonstrated by studies of initial killing and postantibiotic effect and influence of Ca2+ and albumin on these drugs. *Antimicrob. Agents Chemother.* **1991**, 35, 1710.

35. Chen, M.; Shen, N.-X.; Chen, Z.-Q.; Zhang, F.-M.; Chen, Y. Penicilones A–D, Anti-MRSA Azaphilones from the Marine-Derived Fungus Penicillium janthinellum HK1-6. *J. Nat. Prod.* **2017**, 80, 1081-1086.

36. Furi, L.; Ciusa, M. L.; Knight, D.; Di Lorenzo, V.; Tocci, N.; Cirasola, D.; Aragones, L.; Coelho, J. R.; Freitas, A. T.; Marchi, E.; Moce, L.; Visa, P.; Northwood, J. B.; Viti, C.; Borghi, E.; Orefici, G.; Morrissey, I.; Oggioni, M. R.; Consortium, B. Evaluation of Reduced Susceptibility to Quaternary Ammonium Compounds and Bisbiguanides in Clinical Isolates and Laboratory-Generated Mutants of Staphylococcus aureus. *Antimicrob. Agents Chemother.* **2013**, 57, 3488-3497.

37. Zmantar, T.; Miladi, H.; Kouidhi, B.; Chaabouni, Y.; Ben Slama, R.; Bakhrouf, A.; Mahdouani, K.; Chaieb, K. Use of juglone as antibacterial and potential efflux pump inhibitors in Staphylococcus aureus isolated from the oral cavity. *Microb. Pathog.* **2016**, 101, 44-49.

38. Zmantar, T.; Ben Slama, R.; Fdhila, K.; Kouidhi, B.; Bakhrouf, A.; Chaieb, K. Modulation of drug resistance and biofilm formation of Staphylococcus aureus isolated from the oral cavity of Tunisian children. *Braz. J. Infect. Dis.* **2017**, 21, 27-34.

39. Oliveira, A. R. The influence of resveratrol adaptation on resistance to antibiotics, benzalkonium chloride, heat and acid stresses of Staphylococcus aureus and Listeria monocytogenes. *Food Control* **2017**, 73, 1420-1425.

40. Wang, Y.; Damu, G. L. V.; Lv, J.-S.; Geng, R.-X.; Yang, D.-C.; Zhou, C.-H. Design, synthesis and evaluation of clinafloxacin triazole hybrids as a new type of antibacterial and antifungal agents. *Bioorg. Med. Chem. Lett.* **2012**, 22, 5363-5366.

41. Sztanke, K.; Rzymowska, J.; Niemczyk, M.; Dybała, I.; Kozioł, A. E. Novel derivatives of methyl and ethyl 2-(4-oxo-8-aryl-2H-3,4,6,7-tetrahydroimidazo[2,1-c][1,2,4]triazin-3-yl)acetates from biologically active 1-aryl-2-hydrazinoimidazolines: Synthesis, crystal structure and antiproliferative activity. *Eur. J. Med. Chem.* **2006**, 41, 1373-1384.

42. Özdemir, Ü. Ö.; Akkaya, N.; Özbek, N. New nickel(II), palladium(II), platinum(II) complexes with aromatic methanesulfonylhydrazone based ligands. Synthesis, spectroscopic characterization and in vitro antibacterial evaluation. *Inorg. Chim. Acta* **2013**, 400, 13-19.

43. Zani, F.; Incerti, M.; Ferretti, R.; Vicini, P. Hybrid molecules between benzenesulfonamides and active antimicrobial benzo[d]isothiazol-3-ones. *Eur. J. Med. Chem.* **2009**, 44, 2741-2747.

44. Wang, Y.; Li, Y.; Zhang, R.; Huang, L.; He, W. Synthesis and characterization of nanosilica/polyacrylate composite latex. *Polym. Compos.* **2006**, 27, 282-288.

45. Mirzataheri, M.; Mahdavian, A. R.; Atai, M. Nanocomposite particles with core-shell morphology IV: an efficient approach to the encapsulation of Cloisite 30B by poly (styrene-co-butyl acrylate) and preparation of its nanocomposite latex via miniemulsion polymerization. *Colloid Polm. Sci.* **2009**, 287, 725-732.

46. Garay-Jimenez, J. C.; Gergeres, D.; Young, A.; Lim, D. V.; Turos, E. Physical properties and biological activity of poly(butyl acrylate–styrene) nanoparticle emulsions prepared with conventional and polymerizable surfactants. *Nanomed.-Nanotechnol.* **2009**, 5, 443-451.

47. Bosshart, H.; Heinzelmann, M. THP-1 cells as a model for human monocytes. *Ann. Transl. Med.* **2016**, 4, 438-438.

48. Berger, E.; Breznan, D.; Stals, S.; Jasinghe, V. J.; Gonçalves, D.; Girard, D.; Faucher, S.; Vincent, R.; Thierry, A. R.; Lavigne, C. Cytotoxicity assessment, inflammatory properties, and cellular uptake of Neutraplex lipid-based nanoparticles in THP-1 monocyte-derived macrophages. *Nanobiomedicine* **2017**, 4, 1849543517746259-1849543517746259.

49. Klüver, E.; Schulz-Maronde, S.; Scheid, S.; Meyer, B.; Forssmann, W.-G.; Adermann, K. Structure−Activity Relation of Human β-Defensin 3: Influence of Disulfide Bonds and Cysteine Substitution on Antimicrobial Activity and Cytotoxicity. *Biochemistry* **2005**, 44, 9804-9816.

50. André, S.; Washington, S. K.; Darby, E.; Vega, M. M.; Filip, A. D.; Ash, N. S.; Muzikar, K. A.; Piesse, C.; Foulon, T.; O'Leary, D. J.; Ladram, A. Structure–Activity Relationship-based Optimization of Small Temporin-SHf Analogs with Potent Antibacterial Activity. *ACS Chem. Biol.* **2015**, 10, 2257-2266.

51. Kanso, R.; Striegler, S. Multi gram-scale synthesis of galactothionolactam and its transformation into a galactonoamidine. *Carbohydr. Res.* **2011**, 346, 897-904.

52. Striegler, S.; Dittel, M. A Sugar Discriminating Binuclear Copper(II) Complex. *J. Am. Chem. Soc.* **2003**, 125, 11518-11524.

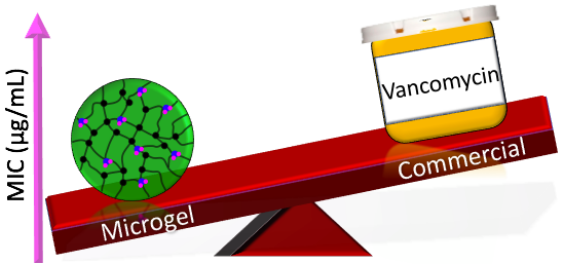
MIC (µg/mL)
Vancomycin
Commercial
Microgel